

Importance of the ocean tide modeling of regional scale in the Earth tide study

Tadahiro Sato

Research Center for Prediction of Earthquakes and Volcanic Eruptions,

Tohoku University

6-6 Aza-Aoba, Aramaki, Aoba-ku, Sendai, 980-8578, Japan

E-mail: tsato@aob.geophys.tohoku.ac.jp

Abstract

This is a summary of an invited talk presented by Sato at the ETS 2008 International Conference 'New Challenges in Earth's Dynamics' that was held in Jena, Germany in September 2008. Main part of the presentation is referred to Sato et al. (2008). Recent improving of the accuracy of the tidal observations and model predictions including the ocean tidal loading (OTL) effects is remarkable. The observed Earth tide data may use to improve the model of the Earth's inside structure, which exhibits a viscoelastic property as well as the laterally inhomogeneous elastic structure. For these, it is essential to improve the accuracy of both the global and regional ocean tide models. An attempt in the region of Southeast Alaska is introduced.

1. Accuracy of the global ocean tide models

Based on the Schwiderski's ocean tide model (Schwiderski, 1980), Schenewerk et al. (2001) computed the ocean tide effects on the vertical components at the IGS-GPS sites in the world, and compared the observed loading effects. A remarkable point of their comparison results is large discrepancy exceeding 3 cm between the observed loading effect of the M_2 constituent and the computed one along the Pacific coast of Alaska.

Thanks to the satellite sea surface altimeters such as TOPEX/Poseidon and Jason-1, the accuracy of the recent global ocean tide models has been much improved compared with those in the 1980s. For example, according to Matsumoto et al. (2000), the vector differences for the M_2 constituent between NAO.99b (Matsumoto et al., 2000) and GOT99.2b (Ray, 1999) are the order of 1 cm or smaller than it almost everywhere in the open seas in the world. Matsumoto et al. (2006) also compared the recent global ocean tide models with the actual ocean bottom pressure gauge (OBPG) measurements in the western Pacific, off Sanriku in northern Japan, and they conclude that the difference between the observation and the five global ocean tide models was less than 1.3 cm in terms of root sum square of the vector differences for eight major tidal constituents (i.e. Q_1 , O_1 , P_1 , K_1 , N_2 , M_2 , S_2 , and K_2). The ocean models they compared are NAO.99 (an old version of NAO.99b), NAO.99b, GOT99.2b, CSR4.0 (Eanes and Bettadpur,

1994), and TPXO.6 (Egbert et al., 1994). Consequently the accuracy of estimation of loading effect has been remarkably improved (e.g. Bos et al., 2002, Sato et al., 2004, Neumeier et al., 2005 for the gravity, and Thomas et al., 2007 for the Global Positioning System (GPS) observation).

However, in contrast to the open seas, accuracy of the global ocean tide models is still questionable in the coastal regions. For example, Southeastern Alaska (SE-AK) is one of the places which show large discrepancy between the observations and the models. The total tidal range at Juneau exceeds 8 m (NOAA website, <http://tidesandcurrents.noaa.gov/index.shtml>), for instance. The analysis results for the 3-years tide gauge data at Juneau indicate that the observed amplitude and phase of M_2 tide are 198.612 ± 0.064 cm and 282.736 ± 0.018 degrees, respectively. On the other hand, those of the five global ocean tide models mentioned above are 133 cm to 353 cm in the amplitude and 206.9 deg to 277.0 deg in the phase at the grid close to Juneau. The differences in the proposed global models are considered to be mainly due to the complex bathymetry and coastline in SE-AK, which are not well represented with the grid size of these global models.

2. Southeast Alaska (SE-AK)

From the point of view of the geodesy and geophysics, SE-AK is an interest place, because very rapid uplift rates exceeding 30 mm/yr at maximum are observed there, which are mainly caused by glacial isostatic adjustment (GIA), including the effects of past and present-day ice melting. During 'Little Ice Age' (LIA), this area was completely covered with glaciers of up to 1.5 km in thickness. Since the middle of the 19th century (i.e. about 250 years ago), when LIA began to wane, this thick ice coverage has rapidly retreated (e.g. Molina, 2008). Therefore, it is considered that, for the effect of the past ice, the melting of the ice of LIA mainly contributes to the observed uplift rates (Larsen et al., 2005 and Larsen et al., 2007).

A joint Japanese-American observation project called ISEA (International geodetic project SouthEastern Alaska) was initiated in 2005 to follow up the work of the University of Alaska Fairbanks (UAF) by adding new geodetic data sets (Miura et al., 2007). In this project, three kinds of geodetic measurements are carried out to study GIA, loading deformation and tidal variations in and around Glacier Bay in SE-AK: (1) the absolute gravity (AG) and relative gravity surveys, (2) surveys with GPS and the establishment of new continuous GPS sites and (3) gravity tide observations. For the GPS, EarthScope (<http://earthscope.org>) continuous GPS data are also used in this project.

In the SE-AK region, the tides including the OTL effects are the major signal in the observed gravity and displacement signals over periods less than seasonal. The OTL effect is 15-30 times larger than the nominal precision of the absolute gravity measurements (i.e. 1-2 μ Gal).

Therefore, precise estimation of the ocean tide effects (i.e. the effects of attraction and loading) is indispensable to increase the accuracy of gravity and GPS observations made to study GIA, when they are carried out over a short period, because it is highly possible that inaccurate OTL correction may easily originate a spurious long-period signal, as pointed out by Penna et al. (2007).

3. Problem in the determination of viscoelasticity of the Earth

Viscoelasticity is important property of the Earth for many geodetic and geophysical phenomena such as the mantle convection, the plate tectonics, the figure of the Earth (J2 and other orders), and the post glacial rebound, etc. Observation of the GIA process gives us the 1st-order information on the viscoelastic property of the Earth. However, we meet a difficulty in the comparison between the observations and the model predictions of the effects of post glacial rebound (PGR), because there exist a problem due to the tradeoff between the viscoelastic parameters, i.e. tradeoff between the magnitude of the upper mantle viscosity and the thickness of the lithosphere in the estimation of the effects of PGR, and also ambiguity of the past ice models, i.e. their extent and thickness of the glaciers (for example, see a paper by Sato et al., 2007, which discusses the GIA problem in Ny-Alesund, Svalbard). In addition to this, present-day ice melting (PDIM) is accelerating in SE-AK as well as other glacier areas in the world, which is considered partly to be the effect of recent 'Global Warming'. GPS and gravity observations in SE-AK clearly detect not only the effect of mass changes in the past ices but also that of PDIM. Error in the estimation of PDIM effects may introduce an additional ambiguity in the estimation of the PGR effects from the observed data.

The magnitude of Earth's viscoelasticity depends on the frequency that is used in the observations (i.e. frequency dependency). Therefore, it is important to constrain the parameters related to the viscoelasticity with the observations over wide frequency bands. If we take a difference from the static (elastic) gravity tidal factor, then the effect of viscoelasticity is estimated at the orders of 0.3% to 0.4% over the frequencies between the semidiurnal and the fortnightly tides (e.g. Lambeck, 1988). For the loading Green's function, its effect is estimated at the order of 0.1% to 0.2% at the frequency band between the semidiurnal and diurnal tides (Okubo and Tsuji, 2001). As well known, the loading Green's function has a nature that it is sensitive to the elastic and/or viscous structure at the depth almost corresponding to the loading distance (i.e. distance between the observation point and the loading point). Therefore, we may have a chance to discuss the viscoelastic structure especially for that of the upper part of the mantle from the OTL effect, because the spatial scale of the variation in the OTL effect is much smaller than that of the body tide.

4. An attempt to improve the regional ocean tide model in SE-AK

The area of our regional model is 5.6 deg. by 7.1 deg. in latitude and longitude, respectively, i.e. 54.5N to 60.1N and 221.9E to 230.0E (see Fig.1, which is taken from Sato et al., 2008). The computation was carried out with a simple method that integrates the simultaneous equations of the Navier-Stokes equation in a coordinate system rotating with the earth and the equation of continuity (Fujii, 1967). The topography and bathymetry are modeled based on the ETOPO2 bathymetry data with the spatial resolution of 2 minutes by 2 minutes (<http://www.ngdc.noaa.gov/mgg/fliers/01mgg04.html>). The model was driven by giving the time variations in the tidal height on the boundary lines at the west and south edges of the model. We used here the NAO.99b model (Matsumoto et al., 2000) for the boundary values. We also took into account the tide gauge data at 12 stations available in the study area, five NOAA continuous tide stations and seven of temporary sites installed by UAF. Their locations are shown in Fig. 1.

The computation is sensitive to the assumed magnitude of the bottom friction (BF). We have searched for the best value in our model computation by changing the BF value within the range of 0.0001 to 0.1 in CGS unit. We may expect that the best BF value should give the amplitude close to the observed one. We have tested at two tide gauge sites, one is faced the open sea and located at the entrance of a long strait. Other one is the back of the strait. The best BF values for the M_2 constituent are slightly different at two sites mainly due to the difference in the geographical condition. However, the difference in the best BF is not so large comparing the range of amplitudes obtained by changing the BF coefficients by the three orders tested here. Therefore, we used here the average value obtained from the test computations for these two sites over the whole sea area of the model considered here, i.e. 0.0029 in CGS unit. We also tested the BF values for the K_1 constituent which has the major amplitude in the diurnal tide. Different from the case of the M_2 constituent, the peak of the curve for the K_1 constituent was broad. Since the wave length of K_1 is longer than that of M_2 , the K_1 wave is not so sensitive to the assumed BF values than that of M_2 .

To examine the effects of the tide gauge data on our modeling in SE-AK, we compared two cases. One does not use the tide gauge data as a boundary condition (Model A) and other uses them (Model B). In general, the amplitudes of Model A are larger than Model B in our computation. The areas show the difference exceeding 100 cm at around Juneau and over the region of Glacier Bay, however, the large amplitude in Model A is suppressed in Model B by introducing the actual tide gauge data into the model computation as expected.

5. Comparison between the observation and prediction

The gravity data were obtained from a Scintrex CG-3M AUTOGRAV gravimeter set at the

Egan library of the University of Alaska, Southeast (UAS) in Juneau. The GPS data obtained at three PBO continuous GPS sites, AB48, AB50 and AB51. PBO is part of a US research facility called EarthScope. To estimate the tidal displacement, we used a PPP method, which was initially introduced by Zumberge et al. (1997). The software used here is 'GpsTools ver. 0.6.3' (Takasu et al., 2005 and Takasu, 2006), which is a GPS/GNSS (Global Navigation Satellite System) analysis software package. The analysis was performed using the BAYTAP-G tidal analysis program (Tamura et al., 1991).

We compared here the predicted tides consisting of the body tide and the OTL effects to the observations. For the body tide, we tested three tidal factors. One is given by Wahr (1981) for the 1066A earth model (Gilbert and Dziewonski, 1975) and other two are given by Dehant, Defraigne and Wahr (1999, here after DDW) for the PREM model (Dziewonski and Anderson, 1981), that is, one for the elastic and hydrostatic (EL-HY) earth and one for the inelastic and non-hydrostatic (IE-NH) earth. Following Farrell's method (1972), we estimated the amplitude and phase of OTL effects by convolving respectively the cosine and sine amplitudes with the loading Green's function over the whole oceans in the world. For the Green's function, we used the PREM earth model (Dziewonski. and Anderson, 1981). In order to represent the topography, a small grid system of 5 by 10 in arc-seconds in latitudinal and longitudinal directions (i.e. about 154 m by 162 m in the respective directions) for the land-sea masking around the observation sites. Fig.2 (This figure taken from Sato et al., 2008) shows the phasor plots of the observations and the predictions.

In Fig. 2, Three kinds of tidal factors are compared. One is by Wahr (1981) for the 1066A earth model (here WAHR), other two for the PREM earth model by Dhant, Defraigne and Wahr (1999), i.e. two of the elastic hydrostatic earth (DDW_EL_HY) and the inelastic and non-hydrostatic earth model (DDW_IE_NH). In each plot, the solid black circles are the observed values with the open sector that shows the observation error estimated by the BAYTAP-G tidal analysis. The Body Tides Amplitude (BTA) shows the amplitude computed using the tidal factors for the DDW_EL-HY model. The phase lag of the body tides was assumed to be zero.

For gravity, Model B is remarkably consistent with the observed M_2 tide and the K_1 constituent is also improved relative to Model A. The actual tide gauge data at Juneau was used in Model B for one of the boundary conditions in the area around EGAN. This may contribute to the improvement. However, for the S_2 and O_1 components, the improvement from including the tide gauge data is relatively small, even though the phase of S_2 is improved. For the displacement, Fig. 2 plots the vector sums of three components NS, EW, and UD. This figure indicates that, except for the K_1 constituent, agreement between the observations and the predictions is generally good in both the amplitude and phase at all the sites compared here.

From Fig. 2, we also see that, the differences between Model A and Model B in the displacements are small compared with the difference in the gravity predictions. For gravity, the attraction part may contribute to the difference in sensitivity. In this connection, for the M_2 tides at the EGAN gravity site, which is located at about 7 km away from the AB50 GPS site, the amplitudes and phases of the attraction part are 3.35 μGal and 185.01 deg. and 2.72 μGal and 185.44 deg. for Model A and Model B, respectively. As shown in Fig.2, for the M_2 constituent, the difference between Model A and B is relatively large at AB51 compared with other sites. Large ocean tide amplitude exceeding 3 m may contribute to this.

It is known that, in GPS time series, the vertical coordinates are much noisier than the horizontal ones, mainly caused by the satellite constellation and by error in the wet zenith delay estimation. The similar situation is shown in Table 1 (This table is taken from Sato et al., 2008), and the UD component shows larger observation errors and generally larger amplitude differences than the horizontal components. On the other hand, Table 1 indicates that, for the semi-diurnal tides, the amplitude difference of the vector sum is smaller than the UD component, and sometimes smaller than the NS and EW components. This means that the magnitude of the tidal displacement vector is determined more accurately than its orientation; the most likely cause for such an error is a small rotation of the tidal displacement vector due to correlations between the coordinate components. However, this clear tendency is not observed in the diurnal tides, suggesting that the observed diurnal tides of the horizontal components might be also affected by the tropospheric error much more than the semi-diurnal tides.

From our comparison results, we may say; (1) Compared with the case only using the global ocean tide models, by taking into account the regional ocean tide effect, the amplitude differences between the observation and the predicted tide in SE-AK is remarkably reduced for both the gravity and displacement (e.g. for the M_2 constituent, 8.5 μGal to 0.3 μGal , and 2.4 cm to 0.1 cm at the AB50 GPS site in Juneau in terms of the vector sum of three components of the north-south, east-west and up-down) , even though the ocean tide loading is large in SE-AK. (2) We have confirmed the PPP (Precise Point Positioning) method, which was used to extract the tidal signals from the original GPS time series, works well to recover the tidal signals. Although the GPS analysis results still contain noise due to the atmosphere and multipath, we may conclude that the GPS observation surely detects the tidal signals with the sub cm accuracy or better than it for some of the tidal constituents. (3) In order to increase the accuracy of the tidal prediction in SE-AK, it is indispensable to improve the regional ocean tide model such as those developed in this study, especially for the phase.

6. Effect of the viscoelasticity

The gravity effect of the loading tide at the EGAN site has a magnitude as large as 6 μGal

for the M_2 tide due to the large ocean tide amplitude, and it is about twice as large as the effect of attraction. We estimated effect of inelasticity on our gravity observation based on a complex Green's function for the inelastic earth given by Okubo and Tsujii (2001), and we obtained a value of $0.05 \mu\text{Gal}$ as the inelastic loading effect on the M_2 constituent at EGAN. On the other hand, the effect of inelasticity on the body tide is estimated at the order of $0.03 \mu\text{Gal}$ from the difference between DDW_EL-HY and DDW_IE-NH (i.e. $23.976 \mu\text{Gal}$ and $24.008 \mu\text{Gal}$ for the former and the latter). The total inelastic effect is to be estimated at the order of $0.08 \mu\text{Gal}$. Unfortunately, its effect is similar in magnitude to the tidal analysis error of our gravity data or slightly larger than it. Therefore, it is difficult to constrain the inelastic effect precisely by the present analysis results, but it should be possible to measure its effect by using an updated well calibrated stable gravimeter better than that used here, because of large amplitude of OTL effects in SE-AK.

Related to a possible source affecting the observed gravity tide, based on the tidal gravity profile obtained in Alaska (north of our study area), Zürn et al. (1976) discussed an effect of geological structure associated with the downgoing lithospheric slab beneath Alaska, and they concluded that this effect on tidal gravity perturbations will be detected when the observation and the estimation of the ocean tide effect achieve an accuracy of 0.1 % and of 1 %, respectively. For the ocean tide effect on M_2 constituent, Fig.2 indicates that, for the estimation by Model B, the difference between the observation and the prediction is about $0.3 \mu\text{Gal}$ and it is at the order of about 1.3 % of the amplitude of predicted body tide (i.e. the ratio of $0.3 \mu\text{Gal}$ to $23.98 \mu\text{Gal}$). Most of the difference is considered to be due to the error in the estimation of the ocean tide effect. Therefore, improvement of the accuracy of the regional ocean tide model in SE-AK is essential for the further discussion of the tidal gravity response observed in SE-AK.

To improve the accuracy of the regional ocean tide model, we have started the following two items; (1) The ocean bottom pressure (OBP) gauge observation has been initiated off Juneau in June 2007. We expect this observation may reveal a possible systematic modification in the existing tide gauge data obtained at the back of the narrow channel. (2) New modeling using more accurate bathymetry data than that by Sato et al. (2008) and considering the spatial variation in the bottom friction, because of very large spatial variation in the speed of tidal currents in the sea area in SE-AK.

7. Additional note

Last, the poster presented by Ito at this symposium is interest related to the title of this symposium 'New Challenges in Earth's Dynamics'. By using a kinematic precise point positioning (KPPP) method, he analyzed the GPS data obtained from 1200 sites of a Japanese

GPS network called GEONET (GPS Earth Observation Network system) operated by GSI (Geographical Survey Institute), and he examined the residuals after subtracting the model tides computed by a GOTIC2 program developed by Matsumoto et al. (2001). In this program, 1066A Earth model and NAO.99b ocean tide model are used to compute the body and ocean loading tides. The obtained M_2 residuals for the vertical tidal displacement indicate that their averaged phase difference is 0.11 degrees across the Japanese islands and most of the sites show a phase delay with respect to the predicted tide. More over, the averaged amplitude ratio of the observation to the prediction is 1.007. From these, he concludes that it may show an Earth's compliant against the response of the Earth obtained from the model computation. Related to this, it may be noted that the 1066A earth model used in GOTIC2 has a soft upper layer compared with other earth models such as PREM model.

Although we should carefully test other models for both the body tide and the OTL effects and check the accuracy of the global ocean tide models, there is a possibility that, from this kind of study, we may reveal the departure of the tidal response of the Earth from that expected from the layered Earth, which is shown for instance by the theoretical estimation by Wang (1991).

Related to this topic, seismic tomography models have revealed the precise 3D image of the Earth's interior. Based on the constructed tomography models, a new image of the mantle dynamics such as mantle plume rising up from the core-mantle boundary is proposed. Basically tomography models are constructed from the body and surface wave data such as travel times and waveforms. However, these data have a defect in the sensitivity to density variations, because the density is a common parameter for both of the P- and S-wave velocities. More over, it is known that the density variations estimated by scaling seismic wave speed models may not be accurate.

To figure out more reliable 3D structure of the Earth's mantle including that of the density, two different kinds of approaches are noticed. One is the utilization of lowest frequency data of the free oscillations of the Earth so called 'gravest seismic normal modes', which depend on lateral variations in density as well as elasticity, because the gravitational restoring force plays an important role to the amplitude and the frequency splitting of these normal modes (e.g. Ritzwoller Lavelly, 1995, Widmer-Schmidrig, 2003, Rosat et al., 2005, 2007). Other is the utilization of the forced oscillations of the Earth such as in the solid Earth tides, because the inside the Earth is deformed by the tidal force as well as its surface, therefore, study of the tidal response of the Earth may be an useful way to reveal in detail about the structure of Earth's inner including the 3D distribution of the density. Such study has been tried by a group of seismologists of America and Canada (Ishii et al., 2008).

An important issue in the tidal tomography is how we can accurately evaluate a possible systematic error in the estimation of the OTL effects and that due to the effect of spatial distribution of the observation sites which are biased toward the continental land areas on the globe. Anyway, improving the ocean tide models of both the global and regional scales is essential to obtain the reliable image of the 3D structure of inside of the Earth from the tidal observations. But, at least, it can be said that the tidal study is coming to a new stage and its importance increases in the study for the Earth's 3D model constructions and related geosciences based on these models.

References

- Bos, M. S., Baker, T. F., Røthing, K., Plag, H.-P., 2002., Testing ocean tide models in the Nordic seas with tidal gravity observations, *Geophys. J. Int.*, 150 (3), 687–694 doi: 10.1046/j.1365-246X.2002.01729.x.
- Dehant, V., Defraigne, P. and Wahr; J. M., 1999. Tides for a convective Earth, *J. Geophys. Res.*, 104, No. B1, 1035-1058.
- Dziwonski, A. D. and D. L. Anderson, 1981. Preliminary Reference Earth Model, *Phys. Earth Planet. Inter.*, 25, 297-356. Eanes, R. J., and S. V. Bettadpur, 1994. Ocean tides from two year of TOPEX/POSEIDON altimetry, *EOS Trans. AGU*, 75(44), Fall Meet. Suppl., 61.
- Eanes, R. J. and S. V. Bettadpur; 1994. Ocean tides from two year of TOPEX/POSEIDON altimetry (abstract), *EOS Trans.*, AGU, 75 (44), Fall Meet., Suppl., 61.
- Egbert, G. D., A. F. Bennette, and M. G. G. Foreman, 1994. TOPEX/POSEIDON tides estimated using a global inverse model, *J. Geophys. Res.*, 99, 24,821 .24,852.
- Farrell, W. E., 1972. Deformation of the Earth by surface loads, *Rev. Geophys. Space Phys.*, 10, 761-797.
- Fujii, Y., 1967. Nmerical Investigations of Tidal Currents in the Kurushima Straits, *Bulle. Kobe Marine Obs.* 179, 1-116.
- Gilbert, F. and Dziewonski, A. M., 1975. An application of normal mode theory to the retrievals of structural parameters and source mechanisms from seismic spectra, *Phil. Trans. R. Soc.*, 278A, 319-328.
- Ishii, M., K., Latychev, J.X., Mitrovica, and J.L., Davis, 2008. Body Tides on a Three-Dimensional Elastic Earth: Toward a Joint Tidal and Seismological Tomography, *Eos Trans. AGU*, 89(53), Fall Meet. Suppl., abstract No. DI11A-08.
- Ito, T., 2008. The high resolution mapping of earth tide responses from GPS network in Japan, Abstract Volume of the ETS 2008 Symposium 'New Challenges in Earth's Dynamics', Jena, Germany, ed. G. Jentzsch, p96.
- Lambeck, K., 1988. *Geophysical geodesy: the slow deformations of the earth*, New York : Oxford University Press.
- Larsen, C. F., 2003. Rapid uplift of southern Alaska caused by recent ice loss, PhD Thesis presented to the Faculty of the University of Alaska Fairbanks.
- Larsen, C. F., R. J. Motyka, J. T. Freymuller, K. A. Echelmeyer, E. R. Ivins, 2005. Rapid viscoelastic uplift southern Alaska caused by post-Little Ice Age glacial retreat, *Earth Planet. Sci. Lett.*, 237, 548-560.
- Larsen, C. F., R. J. Motyka, A. A. Arendt, K. A. Echelmeyer, and P. E. Geissler, 2007. Glacier changes in southeast Alaska and northwest British Columbia and contribution to sea level

- rise, 2007, *J. Geophys. Res.*, VOL. 112, F01007, doi:10.1029/2006JF000586.
- Matsumoto, K., T. Sato, T. Takanezawa, and M. Ooe, 2001. A Program for Computation of Oceanic Loading Effects, *J. Geodetic Soc. Japan*, Vol.47, No.1, 243-254.
- Matsumoto, K., Takanezawa, T. and Ooe, M., 2000. Ocean tide models developed by assimilating TOPEX/Poseidon altimeter data into hydro-dynamical model: A global model and a regional model around Japan, *J. Oceanogr.*, 56, 567-581.
- Matsumoto, K., Sato, T., Fujimoto, H., Tamura, Y., Nishino, M., Hino, R., Higashi, T. and Kanazawa, T., 2006. Ocean bottom pressure observation off Sanriku and comparison with ocean tide models, altimetry, and barotropic signals from ocean models, *Geophys. Res. Lett.*, 33, L16602, doi: 10.1029/2006GL026706.
- Miura, S., Sato, T., Freymuller, J. T., Kaufman, M., Cross, R., Sun, W., and Fujimoto, H., 2007. Geodetic measurements for monitoring rapid crustal uplift in southeast Alaska caused by post-glacial rebound –Outline of the project–. *Proc. 7th International Conference on Global Change: Connection to Arctic (GCCA-7)*, ed. by H. L. Tanaka, International Arctic Research Center, Univ. Alaska Fairbanks, 95–97.
- Molnia, B.F., 2008. *Glaciers of North America -- Glaciers of Alaska*, in Williams, R.S., Jr., and Ferrigno, J.G., eds., *Satellite image atlas of glaciers of the world: U.S. Geological Survey Professional Paper 1386-K*, 525 p.
- Neumeyer, J., del Pino, J., Dierks O., Sun, H.P., and Hartmut, P., 2005. Improvement of ocean loading correction on gravity data with additional tide gauge measurements, *J. Geody.*, Vol. 40, No.1, 104-111.
- Okubo, S. and Tsuji, D., 2001. Complex Green's Function for Diurnal/Semidiurnal Loading Problem, *J. Geod. Soc. of Japan*, Vol.47, No.1, 225-230.
- Penna, N. T., M. A. King, and M. P. Stewart, 2007. GPS height time series: Short-period origins of spurious long-period signals, *J. Geophys. Res.*, 112, B02402 (doi:10.1029/2005JB004047).
- Ray, R. D., 1999. A global ocean tide model from TOPEX/POSEIDON altimetry: GOT99.2b, Tech. Memo. 209478, NASA Goddard Space Flight Cent., Greenbelt, Md.
- Ritzwoller, M., and E. M. Lavelly, 1995. Three-dimensional seismic models of the Earth's mantle, *Rev. Geophys.*, 33, 1 – 66.
- Rosat, S., T. Sato, Y. Imanishi, J. Hinderer, Y. Tamura, H. McQueen, and M. Ohashi, 2005. High resolution analysis of the gravest seismic normal modes after the 2004 Mw=9 Sumatra Earthquake using superconducting gravimeter data, *Geophys. Res. Lett.*, **32**, L13304, doi:10.1029/2005GL023128, 2005.
- Rosat, S., S. Watada, and T. Sato, 2007. Geographical variations of the ${}_0S_0$ normal mode amplitude: predictions and observations after the Sumatra-Andaman Earthquake, *Earth*

- Planets Space, **59**, 307–311.
- Sato, T., Tamura, Y., Matsumoto, K., Imanishi, Y. and McQueen, H., 2004. Parameters of the fluid core resonance inferred from superconducting gravimeter data, *J. Geodyn.*, **38**, 375-389.
- Sato, Tadahiro, Jun'ichi Okuno, Jacques Hinderer, Daniel S. MacMillan, Hans-Peter Plag, Olivier Francis, Reinhard Falk, and Yoichi Fukuda, 2006. A geophysical interpretation of the secular displacement and gravity rates observed at Ny-Ålesund, Svalbard in the Arctic - Effects of post-glacial rebound and present-day ice melting -, *G. J. Int.*, **165.**, 729-743, doi: 10.1111/j.1365-246x.2006.02992.x.
- T. Sato, S. Miura, Y. Ohta, H. Fujimoto, W. Sun, C.F. Larsen, M. Heavner, A.M. Kaufman, J.T. Freymueller, 2008. Earth tides observed by gravity and GPS in southeastern Alaska, *J. Geodyn.*, **46**, 78–89.
- Schenewerk, M. S., J. Marshall and W. Dillingar (2001), Vertical Ocean-loading Deformations Derived from a Global GPS Network, *J. Geod. Soc. Japan*, Vol.47, No.1, 237-242.
- Schwiderski, E. W. (1980), On charting global ocean tides, *Rev. Geophys. Space Phys.*, **18**, 243-268.
- Takasu, T., and Kasai, S., 2005. Development of precise orbit/clock determination software for GPS/GNSS, *Proce. the 49th Space Sciences and Technology Conference*, Hiroshima, Japan (in Japanese), 1223-1227.
- Takasu, T., 2006. High-rate Precise Point Positioning: Detection of crustal deformation by using 1-Hz GPS data, *GPS/GNSS symposium 2006*, Tokyo, 52-59.
- Tamura Y., Sato, T., Ooe, M. and Ishiguro, M., 1991. A procedure for tidal analysis with a Bayesian information criterion, *Geophys. J. Int.*, **104**, 507-516.
- Thomas, I. D., King, M. A., Clarke, P. J., 2007. A comparison of GPS, VLBI and model estimates of ocean tide loading displacements, *J. Geodesy*, **81(5)**, 359-268.
- Wahr, J. M., 1981. Body tides of an elliptical, rotating, elastic and oceanless Earth, *Geophys. R. Astron. Soc.*, **64**, 677-703.
- Wang, R., 1991. Tidal deformations of a rotating, spherically symmetric, visco-elastic and laterally heterogeneous Earth, Ph.D. Thesis, Univ. of Kiel, Kiel, Germany.
- Widmer-Schmidrig, R., 2003. What can superconducting gravimeters contribute to normal mode seismology?, *Bull. Seism. Soc. Am.*, **93(3)**, 1370–1380.
- Zumberge, J. F., Heflin, M. B., Jefferson, D. C., Watkins, M. M., and Webb, F. H., 1997. Precise point positioning for the efficient and robust analysis of GPS data from large networks, *J. Geophys. Res.*, **102 (B3)**, 5005-5017.
- Zürn, W., Beaumont, C. and Slichter, L. B., 1976. Gravity tides and ocean loading in southern Alaska, *J. Geophys. Res.*, Vol. 81, No. 26, 4923-4932.

Table 1. Amplitude differences between the observed tidal displacements from GPS and the predictions for the four constituents of O_1 , K_1 , M_2 , and S_2 . In this table, the predicted tides were computed with a combination of the Green's function for the elastic PREM given by Dehant, Defraigne and Wahr (1999), NAO.99b global tide model and the Model B regional tide model (see subsection 4). Results for three GPS sites of AB48, AB50 and AB51 are shown. Unit of the amplitude difference: cm. VSM: Vector sum of the NS, EW and UD components.

Site	Wave	Amplitude difference				Observation error			
		NS	EW	UD	VSM	NS	EW	UD	VSM
AB48									
	O_1	0.38	0.12	0.49	0.50	0.03	0.03	0.04	0.06
	K_1	0.50	0.89	1.43	1.57	0.03	0.03	0.05	0.06
	M_2	0.02	0.08	0.59	0.08	0.03	0.03	0.06	0.07
	S_2	0.38	0.24	0.82	0.43	0.03	0.03	0.05	0.07
AB50									
	O_1	0.10	0.14	0.24	0.27	0.02	0.10	0.03	0.11
	K_1	0.25	1.01	0.78	0.89	0.02	0.10	0.03	0.10
	M_2	0.11	0.10	0.23	0.08	0.02	0.03	0.04	0.05
	S_2	0.77	0.40	0.58	0.38	0.02	0.03	0.04	0.05
AB51									
	O_1	0.02	0.10	0.31	0.32	0.01	0.01	0.03	0.03
	K_1	0.23	0.34	0.25	0.29	0.02	0.02	0.03	0.04
	M_2	0.08	0.10	0.37	0.31	0.02	0.02	0.03	0.04
	S_2	0.27	0.25	0.54	0.33	0.02	0.02	0.03	0.04

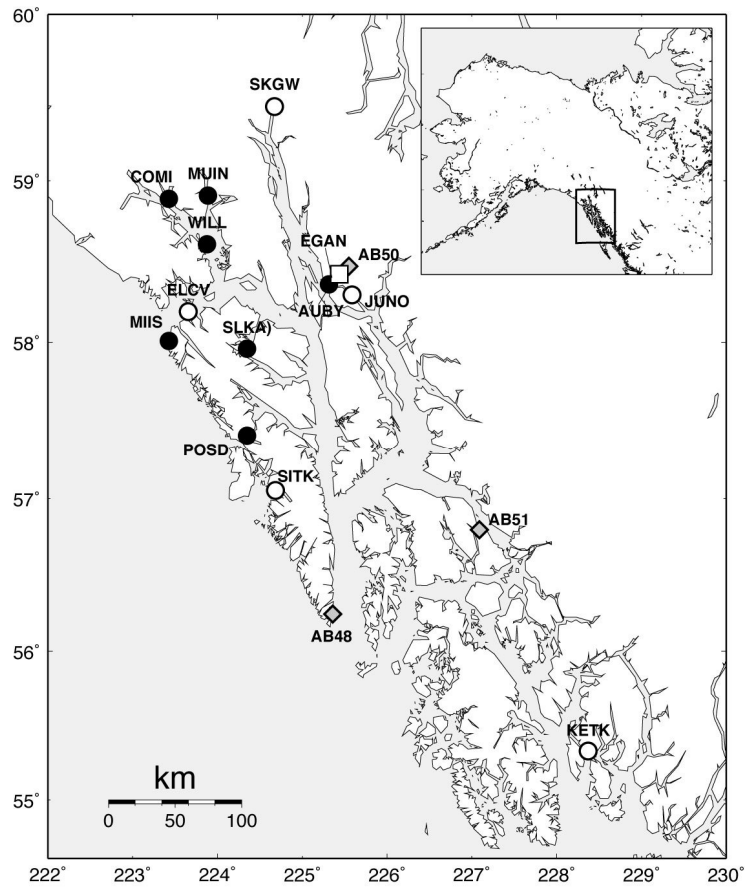


Fig. 1. Locations of the observation sites used in this study. An open square, a diamond, open circles, and closed circles indicate the tidal gravity, continuous GPS, continuous tide gauges, and temporal tide gauges installed by UAF (Larsen, 2003), respectively.

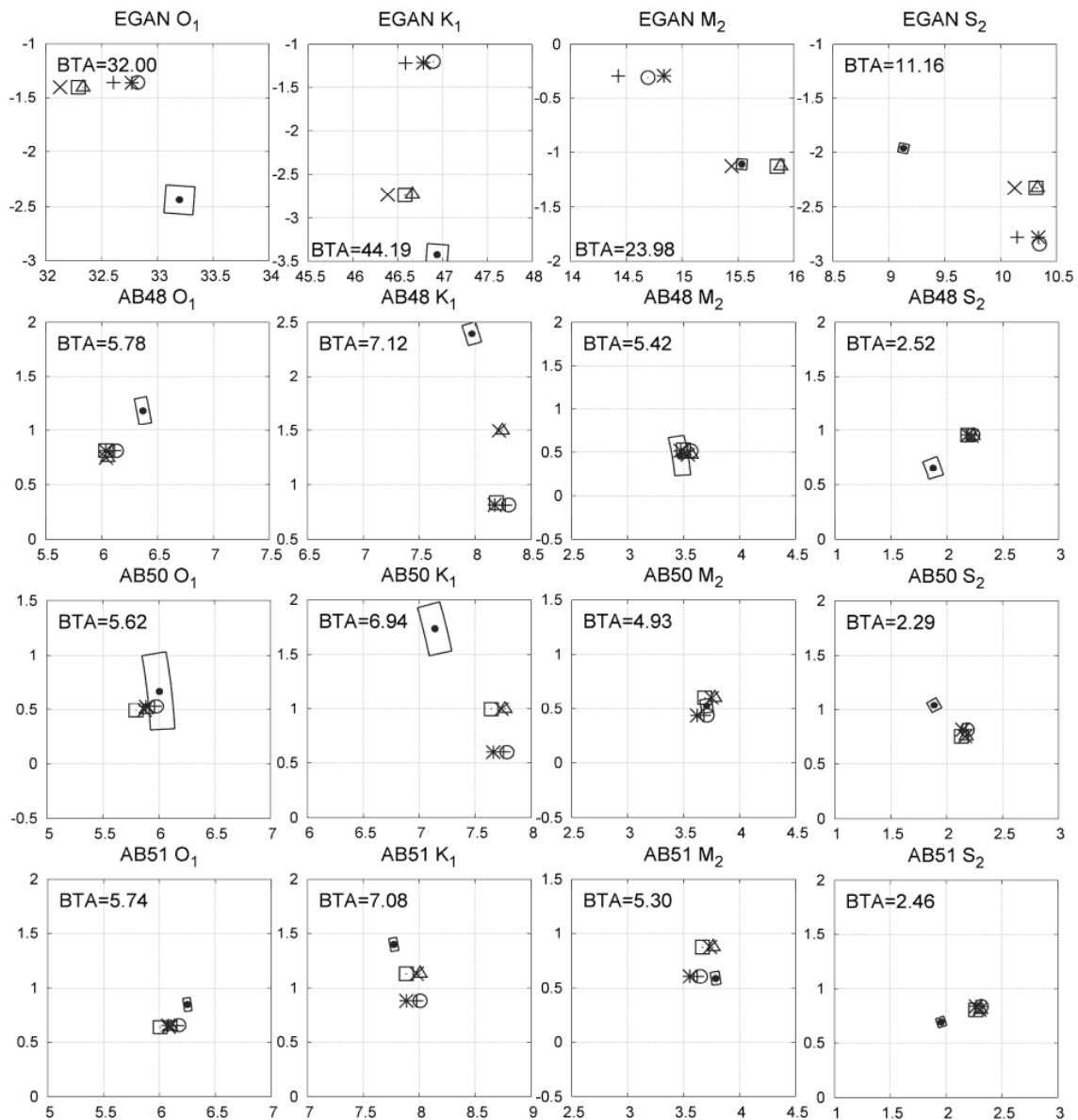


Fig. 2. Phasor plots for the observed and predicted tides at four sites of EGAN (gravity) and AB48, AB50, and AB51 (displacement). Units of both the horizontal and vertical axes are in μGal and cm for the gravity and displacement, respectively. For the displacement, the vector sums of three components of NS, EW and UD are plotted. The six combinations of the predicted body tide and the regional ocean tide model (Model A or B) are plotted with the following symbols; (1) Cross denoted with '+': Predictions from WAHR and Model A, (2) Stars: DDW_EL_HY and Model A; (3) Open circle: DDW_IE_NH and Model A, (4) Cross denoted with 'x': WAHR and Model B, (5) Open square: DDW_EL_HY and Model B, and (6) Open triangle: DDW_IE_NH and Model B. See Section 5 of the text for the abbreviations of the body tides.

BLANK PAGE